

Effects of hydrostatic pressure on the electron g_{\parallel} factor and g -factor anisotropy in GaAs-(Ga, Al)As quantum wells under magnetic fields

This article has been downloaded from IOPscience. Please scroll down to see the full text article.

2008 J. Phys.: Condens. Matter 20 465220

(<http://iopscience.iop.org/0953-8984/20/46/465220>)

View [the table of contents for this issue](#), or go to the [journal homepage](#) for more

Download details:

IP Address: 129.252.86.83

The article was downloaded on 29/05/2010 at 16:36

Please note that [terms and conditions apply](#).

Effects of hydrostatic pressure on the electron g_{\parallel} factor and g -factor anisotropy in GaAs–(Ga, Al)As quantum wells under magnetic fields

N Porrás-Montenegro^{1,2}, C A Duque^{2,3}, E Reyes-Gómez³ and L E Oliveira^{2,4}

¹ Departamento de Física, Universidad del Valle, AA 25360, Cali, Colombia

² Instituto de Física, UNICAMP, CP 6165, Campinas, São Paulo, 13083-970, Brazil

³ Instituto de Física, Universidad de Antioquia, AA 1226, Medellín, Colombia

⁴ Inmetro, Campus de Xerém, Duque de Caxias, Rio de Janeiro, 25250-020, Brazil

Received 5 July 2008, in final form 9 September 2008

Published 27 October 2008

Online at stacks.iop.org/JPhysCM/20/465220

Abstract

The hydrostatic-pressure effects on the electron-effective Landé g_{\parallel} factor and g -factor anisotropy in semiconductor GaAs–Ga_{1-x}Al_xAs quantum wells under magnetic fields are studied. The g_{\parallel} factor is computed by considering the non-parabolicity and anisotropy of the conduction band through the Ogg–McCombe effective Hamiltonian, and numerical results are displayed as functions of the applied hydrostatic pressure, magnetic fields, and quantum-well widths. Good agreement between theoretical results and experimental measurements in GaAs–(Ga, Al)As quantum wells for the electron g factor and g -factor anisotropy at low values of the applied magnetic field and in the absence of hydrostatic pressure is obtained. Present results open up new possibilities for manipulating the electron-effective g factor in semiconductor heterostructures.

(Some figures in this article are in colour only in the electronic version)

1. Introduction

The interaction between the electron spin and its solid-state environment has been the subject of a considerable amount of work in the last few years [1–6]. These studies have been motivated on one hand by the theoretical interest in elucidating the physical properties of the spin-based electronic systems, and on the other hand by the potential and real applications in the design and construction of optoelectronic and spintronic devices. The study of the behavior of the electron spin is a fundamental keystone for the development of quantum computers. At the same time, the coupling of the electron spin with an external magnetic field is of great importance to obtain coherent spin states in order to avoid losses in the spin-based transport information. In semiconductor heterostructures, this may be achieved by manipulating the electron-effective g factor of the system, i.e. by controlling the spin dynamics and spin relaxation in those systems. The electron-effective

g factor is then of relevance in a series of applications based on magneto-optical and magnetotransport studies of semiconductor heterostructures. Therefore, a great deal of experimental and theoretical work has been devoted to the understanding of the properties of the electron-effective g factor in such semiconductor systems [7–17]. In addition, an applied hydrostatic pressure may be used to tailor the electron-spin response in a wide variety of semiconductor systems. In GaAs–(Ga, Al)As quantum wells (QWs), for example, it is well known that an applied hydrostatic pressure modifies the electronic band structure, and consequently leads to changes in the electron and hole energy states causing direct and indirect electron–hole transitions [18–20]. Moreover, such effects may show up in the electron-effective g factor, opening up new possibilities to tune the electron-spin dynamics and relaxation in semiconductor heterostructures.

In bulk Ga_{1-x}Al_xAs the electron-effective g factor may be investigated within the $\mathbf{k} \cdot \mathbf{p}$ framework [7–10], a tool which

has proven to be of great value to understand many optical and electrical properties of such materials. In QWs the electron g factor has been measured by using various experimental techniques [11–15]. From the theoretical point of view, however, investigations of the properties of the effective Landé factor in QWs require the inclusion of the non-parabolicity and anisotropy of the conduction band in the theoretical framework by using multiband schemes [16, 17], or equivalently by using phenomenological models such as the Ogg–McCombe effective Hamiltonian [21, 22]. Most of these works have been mainly carried out without the consideration of hydrostatic-pressure effects, although such effects play a relevant role in the study of skyrmions in the limit of zero g factor [23].

The purpose of the present work is to perform a predictive study of the hydrostatic-pressure and magnetic-field effects on the electron g_{\parallel} factor and g -factor anisotropy in GaAs–(Ga, Al)As QWs by taking into account the anisotropy and non-parabolicity of the conduction band. Here we extend and complement a previous study on the hydrostatic-pressure effects on the electron-effective g_{\perp} factor in GaAs–(Ga, Al)As QWs under in-plane magnetic fields [24]. In section 2 we describe the motion of a conduction electron in a GaAs–(Ga, Al)As QW under a hydrostatic pressure and a growth-direction applied magnetic field. Section 3 presents results and discussions, and conclusions are in section 4.

2. Theoretical framework

We study the motion of a conduction electron in a GaAs–(Ga, Al)As QW grown along the z axis under growth-direction applied magnetic fields ($\mathbf{B} = B\hat{\mathbf{z}}$) and hydrostatic pressure. In the effective-mass approximation and taking into account the non-parabolicity and anisotropy effects on the conduction band, the Ogg–McCombe effective Hamiltonian [21, 22] may be written as

$$\begin{aligned} \hat{H} = & \frac{\hbar^2}{2} \hat{\mathbf{K}} \frac{1}{m} \hat{\mathbf{K}} + \frac{1}{2} g \mu_B \hat{\sigma}_z B + V + a_1 \hat{\mathbf{K}}^4 + \frac{a_2}{l_B^4} \\ & + a_3 \left[\left\{ \hat{K}_x^2, \hat{K}_y^2 \right\} + \left\{ \hat{K}_y^2, \hat{K}_z^2 \right\} + \left\{ \hat{K}_z^2, \hat{K}_x^2 \right\} \right] \\ & + a_4 B \hat{\mathbf{K}}^2 \hat{\sigma}_z + a_5 \left\{ \hat{\sigma} \cdot \hat{\mathbf{K}}, \hat{K}_z B \right\} + a_6 B \hat{\sigma}_z \hat{K}_z^2, \end{aligned} \quad (1)$$

where $\hat{\mathbf{K}} = -i\nabla + \frac{e}{\hbar c} \hat{\mathbf{A}}$, $\hat{\mathbf{A}}$, and $\hat{\sigma}$ are the generalized momentum operator, the magnetic vector potential, and a vector with Pauli matrices as components, respectively, whereas μ_B and $l_B = \sqrt{\frac{\hbar c}{eB}}$ are the Bohr magneton and the Landau length, respectively. The anticommutator between the \hat{a} and \hat{b} operators is represented as $\{\hat{a}, \hat{b}\} = \hat{a}\hat{b} + \hat{b}\hat{a}$. The phenomenological parameters a_1 , a_2 , a_3 , a_4 , a_5 , and a_6 are constants which are, in principle, dependent on the hydrostatic pressure and aluminum concentration in the barriers. Due to the absence of experimental measurements devoted to establishing such dependences, we have used the values obtained by a fitting with magnetospectroscopic measurements reported by Golubev *et al* [25] in bulk GaAs. The growth-direction position-dependent conduction-electron-effective mass m and Landé factor g , together with the electron-confining potential V , are taken as z -dependent

functions and also considered to be dependent on the hydrostatic pressure P and aluminum concentration x in the $\text{Ga}_{1-x}\text{Al}_x\text{As}$ barrier of the heterostructure, as detailed in [24]. The Dresselhaus cubic spin–orbit interaction [26] is not considered here, due to its minor contribution to the effective g factor in GaAs–(Ga, Al)As heterostructures [27].

As \hat{H} does not explicitly depend on the x -coordinate, the eigenfunctions of the Hamiltonian (1) may be chosen as

$$\Psi(\mathbf{r}) = \begin{pmatrix} \Phi^{(+)}(y, z) \\ \Phi^{(-)}(y, z) \end{pmatrix} e^{ik_x x}, \quad (2)$$

and by introducing $y' = y - l_B^2 k_x$, and the annihilation $\hat{a} = \frac{1}{\sqrt{2}}[\frac{y'}{l_B} + ik_y l_B]$ and creation \hat{a}^\dagger operators, the Ogg–McCombe Hamiltonian may be transformed into

$$\hat{H} = \hat{\mathcal{H}}_0 + \hat{\mathcal{W}}, \quad (3)$$

where

$$\hat{\mathcal{H}}_0 = \begin{pmatrix} \hat{\mathcal{H}}_0^+ & 0 \\ 0 & \hat{\mathcal{H}}_0^- \end{pmatrix}, \quad (4)$$

$$\hat{\mathcal{H}}_0^\pm = \hat{k}_z \hat{\beta}^\pm \hat{k}_z + \hat{k}_z^2 a_1 \hat{k}_z^2 + \hat{U}^\pm, \quad (5)$$

$$\hat{\beta}^\pm = \frac{\hbar^2}{2m(z)} \pm (a_4 + 2a_5 + a_6)B + 4 \frac{a_1 + a_3}{l_B^2} \hat{N}, \quad (6)$$

$$\begin{aligned} \hat{U}^\pm = & \frac{a_3 + 4a_1}{l_B^4} \hat{N}^2 + \frac{2}{l_B^2} \left[\frac{\hbar^2}{2m(z)} \pm a_4 B \right] \hat{N} \\ & + \frac{a_2 - \frac{3}{4}a_3}{l_B^4} \pm \frac{1}{2} g(z) \mu_B B + V(z), \end{aligned} \quad (7)$$

and $\hat{N} = \hat{a}^\dagger \hat{a} + \frac{1}{2}$. The operator $\hat{\mathcal{W}}$ in equation (3) is given by

$$\hat{\mathcal{W}} = \begin{pmatrix} \hat{\mathcal{W}}_{11} & \hat{\mathcal{W}}_{12} \\ \hat{\mathcal{W}}_{21} & \hat{\mathcal{W}}_{22} \end{pmatrix}, \quad (8)$$

where

$$\hat{\mathcal{W}}_{22} = \hat{\mathcal{W}}_{11} = -\frac{a_3}{2l_B^4} (\hat{a}^{\dagger 4} + \hat{a}^4), \quad (9)$$

and

$$\hat{\mathcal{W}}_{21} = \hat{\mathcal{W}}_{12}^\dagger = \left[-\frac{\sqrt{2}}{l_B} (2a_5 B \hat{a} \hat{k}_z) \right]^\dagger. \quad (10)$$

The characteristic problem for $\hat{\mathcal{H}}_0$ may be solved analytically, and the operator $\hat{\mathcal{W}}$ only contributes with a very small correction to the energy levels [28]. Therefore, in the case of the \mathbf{B} magnetic field in the growth direction, one may use perturbation theory to find the solution of the Schrödinger equation. The electron-effective Landé g_{\parallel} factor (the electron-effective g factor along the z -axis) in the GaAs–(Ga, Al)As heterostructure may be defined as

$$g_{\parallel} = \frac{E_0^{(+)} - E_0^{(-)}}{\mu_B B}, \quad (11)$$

where $E_0^{(+)}$ and $E_0^{(-)}$ are the energies corresponding to the spin-up and spin-down ground-state eigenfunctions in equation (2), respectively. One may note that the hydrostatic-pressure dependence on the eigenvalues $E_n^{(+)}$ and $E_n^{(-)}$ of (3) is included via the hydrostatic-pressure dependence of the electron-effective mass and g factor in each QW building material, as well as on the QW-confining potential (see [24] for details).

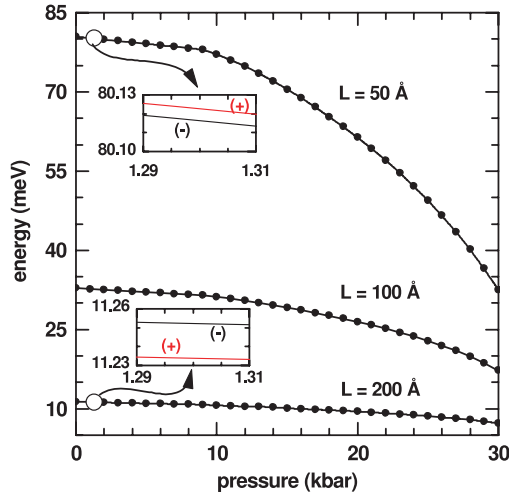


Figure 1. Electron spin-up (dots) and spin-down (solid lines) Landau energy levels in GaAs–Ga_{0.7}Al_{0.3}As QWs with $L = 50 \text{ \AA}$, 100 \AA , and 200 \AA , as functions of the hydrostatic pressure, for $B = 1 \text{ T}$.

3. Results and discussion

The energies of the first spin-up (+) and spin-down (–) Landau levels in GaAs–Ga_{0.7}Al_{0.3}As QWs, as functions of the hydrostatic pressure, are displayed in figure 1 for different values of the well widths. The effect of the hydrostatic pressure is to diminish the energy of the Landau levels, as expected due to the decrease of the confining potential as the pressure applied over the system is increased [20, 24, 29]. The applied magnetic field breaks up the spin degeneracy, as is clearly displayed in the two insets, where we have shown the energies of the spin-up and spin-down ground-state Landau levels for two different values of the QW width, indicating a sign change of the effective Landé factor as the well width is increased. For all values of the QW width considered in the present calculations, the g_{\parallel} factor behave as a growing function of the hydrostatic pressure and applied magnetic field. One may note that the hydrostatic-pressure dependence of the g_{\parallel} factor is more significant for the widest wells than for the narrowest ones (cf figure 2). This behavior may be understood in terms of the hydrostatic-pressure and aluminum dependences of the effective Landé factor in bulk Ga_{1-x}Al_xAs. According to the $\mathbf{k} \cdot \mathbf{p}$ analysis, the electron Landé g factor in a III–V material is given by [8, 15]

$$g = g_0 \left[1 - \frac{\Pi^2}{3} \frac{\Delta_0}{E_g^{\Gamma} [E_g^{\Gamma} + \Delta_0]} + \delta_g \right], \quad (12)$$

where $g_0 = 2.0023$ is the free-electron Landé factor, $\Pi^2 = \frac{2}{m_0} |\langle S | \hat{p}_x | X(\Gamma_5^v) \rangle|^2$ is the square of the interband matrix element associated with the coupling between the s states of the Γ_6^c conduction band with the valence states Γ_5^v (Γ_8^v and Γ_7^v), $E_g^{\Gamma} = E(\Gamma_6^c) - E(\Gamma_8^v)$ is the fundamental gap, $\Delta_0 = E(\Gamma_8^v) - E(\Gamma_7^v)$ is the split-off valence gap and δ_g accounts for the remote-band effects on the electron Landé factor [24]. The effects of the applied hydrostatic pressure on the electron g factor are considered through

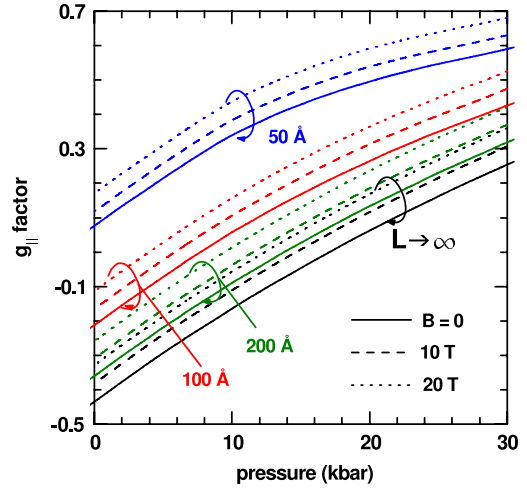


Figure 2. Electron g_{\parallel} factor as a function of the hydrostatic pressure in GaAs–Ga_{0.7}Al_{0.3}As QWs with $L = 50 \text{ \AA}$, 100 \AA , 200 \AA , and the bulk GaAs limit ($L \rightarrow \infty$). Solid, dashed, and dotted lines correspond to $B = 0$, 10 T , and 20 T , respectively.

the hydrostatic-pressure dependences of the different energy gaps and interband matrix elements in the corresponding material [24]. For bulk Ga_{1-x}Al_xAs it has been proven that the fundamental gap E_g^{Γ} is a growing linear function of the hydrostatic pressure, for which the slope (pressure coefficient) is positive and independent of the aluminum concentration at low temperatures [30]. The split-off valence gap Δ_0 , however, does not depend on the hydrostatic pressure [31]. With respect to the square of the interband matrix element, the hydrostatic-pressure dependence of Π in GaAs–(Ga, Al)As QWs and superlattices has been extensively studied both from the experimental [32] and theoretical [33] points of view. According to such studies, the matrix element Π is almost constant on increasing the hydrostatic pressure, but for hydrostatic-pressure values close to the Γ – X crossover a rapid decrease of Π takes place, a fact which may be understood in terms of the mixing between the Γ_6^c and X_6^c conduction-electron states. Here we have considered, for simplicity, the matrix element Π as independent of the applied pressure. Such an approximation is only rigorously valid for hydrostatic pressures far from the Γ – X crossover. As the interband matrix element decreases for hydrostatic pressures beyond the crossover, an increase in the g factors corresponding to each QW material is expected to occur (see equation (12)), leading to a slight correction of the effective Landé factor associated with the heterostructure. We have also considered the remote-band contribution δ_g as independent of the applied pressure. On the other hand, both the fundamental and split-off energy gaps increase and Π^2 decreases as the aluminum concentration is increased [24]. Thus, by combining these facts with expression (12), one may note that the hydrostatic-pressure dependence of the g factor is more remarkable in the GaAs well than in the Ga_{1-x}Al_xAs barriers, and therefore the electron-effective g_{\parallel} factor is more sensitive to the hydrostatic pressure in the limit of $L \rightarrow \infty$ than when $L = 50 \text{ \AA}$. It is apparent from figure 2 that the g_{\parallel} factor increases as the magnetic field is increased. This fact is clearly displayed

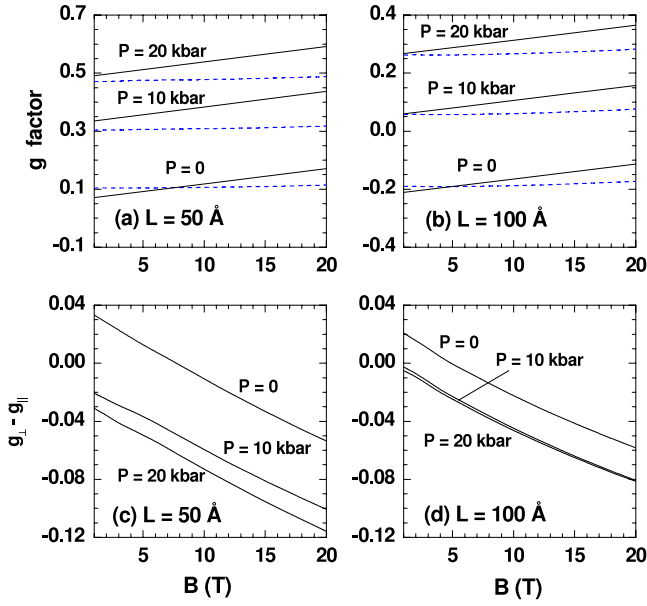


Figure 3. Magnetic-field dependence of the electron g factor ((a) and (b)) and g -factor anisotropy ((c) and (d)) in GaAs–Ga_{0.7}Al_{0.3}As QWs with $L = 50$ and 100 Å for three different values of the hydrostatic pressure. Solid and dashed lines in (a) and (b) correspond to electron g_{\parallel} (growth-direction applied magnetic field) and g_{\perp} (in-plane applied magnetic field [24]) factors, respectively.

in figures 3(a) and (b), where we have shown the magnetic-field dependence of the electron-effective g_{\parallel} factor (solid lines) in GaAs–Ga_{0.7}Al_{0.3}As QWs for different values of the well width and the applied hydrostatic pressure. We also display the numerical results for the g_{\perp} factor (dashed lines) in GaAs–Ga_{0.7}Al_{0.3}As QWs obtained according to [24]. In both cases (g_{\parallel} or g_{\perp}), the electron-effective Landé factor is a linear function of the applied magnetic field, with a positive slope which is independent of the hydrostatic pressure and QW width. However, a more pronounced dependence on the applied magnetic field is observed in the case of the g_{\parallel} factor. As we have pointed out [24, 34], in GaAs–(Ga, Al)As QWs under in-plane magnetic fields the electron momentum k_z along the magnetic-field direction is a constant of motion, and at low temperatures no important contributions of k_z to the electron states and g_{\perp} are expected to occur. The $k_z = 0$ approximation was successfully used to investigate the behavior of the g_{\perp} factor in semiconductor heterostructures [24, 34–36], and contributions to the electron-effective Landé factor of the terms proportional to a_5 and a_6 in the Ogg–McCombe Hamiltonian (which are also proportional to the applied magnetic field) are negligible. One may expect, therefore, a slight dependence of g_{\perp} on the magnetic field. In contrast, the terms proportional to a_5 and a_6 in (1) are of fundamental importance in the electron dynamics in QWs under growth-direction applied magnetic fields [37], and therefore they have a great influence on the energy spectrum, leading to a stronger magnetic-field dependence of the effective g_{\parallel} factor than of the g_{\perp} Landé factor. Previous experimental work [11–13] on GaAs–Ga_{0.7}Al_{0.3}As QWs indicates that, in the absence of hydrostatic pressure and for low values of the applied magnetic field, the

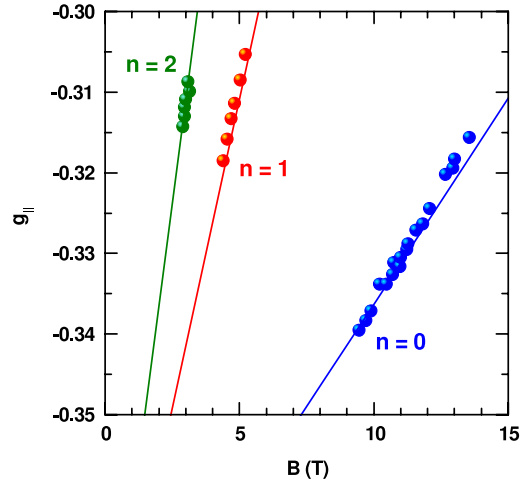


Figure 4. Magnetic-field dependence of the electron g_{\parallel} factor corresponding to sample 2 (solid dots) of Dobers *et al* [38] associated with the $n = 0, 1,$ and 2 Landau levels, in the absence of hydrostatic pressure. Present $P = 0$ theoretical results (solid curves) correspond to an $L = 250$ Å GaAs–Ga_{0.65}Al_{0.35}As QW as in the experimental measurements [38].

electron g_{\perp} factor is larger than the g_{\parallel} factor, with theoretical studies confirming these results [34, 37]. However, for a sufficiently larger magnetic field and hydrostatic pressure this behavior may be reversed and a g_{\parallel} factor larger than the g_{\perp} may be obtained, as we have displayed in figure 3. The anisotropy in the g factor is basically due to the anisotropy imposed by the confining potential. Of course, different orientations of the applied magnetic field with respect to the growth direction lead to different localization properties of the electron wavefunction, energy spectrum, and effective g factor. By changing the geometrical parameters of the heterostructure, the applied magnetic field or the hydrostatic pressure, it is possible to change the electronic properties of the system, and therefore to revert the anisotropy of the electron-effective Landé factor.

We have also compared in figure 4 the present theoretical results for the magnetic-field dependence of the effective g_{\parallel} factor, in the absence of hydrostatic pressure, with the experimental data reported by Dobers *et al* [38], who studied the properties of the effective Landé factor in a GaAs–Ga_{0.65}Al_{0.35}As heterostructure (sample 2 in [38]) under magnetic fields applied perpendicular to the plane of the two-dimensional electron gas at $P = 0$. Present calculations (cf figure 4) of the g_{\parallel} factor as a function of the applied magnetic field clearly agree quite well with the experimental measurements by Dobers *et al* [38].

In figure 5 we display the GaAs–Ga_{0.65}Al_{0.35}As QW-width dependence of g_{\parallel} (solid lines) for $B = 1$ T and for three different values of the hydrostatic pressure. The theoretical procedure to compute the g_{\perp} factor was described in [24]. One may note the excellent agreement between present theoretical results and experimental measurements [11–13] at low values of the applied magnetic field and in the absence of hydrostatic pressure. An increase of the applied hydrostatic pressure leads to an increase of the electron-effective Landé factor in both

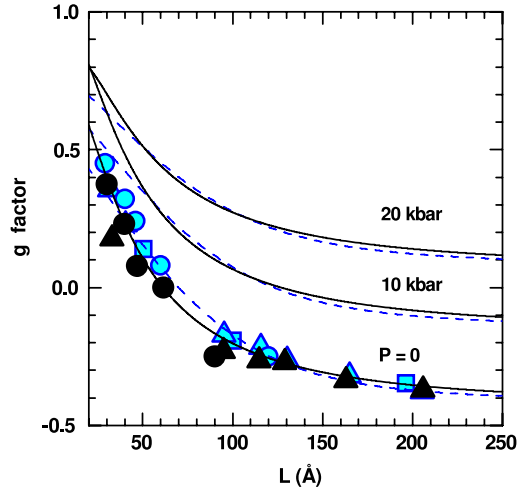


Figure 5. Electron g factor as a function of the well width in GaAs–Ga_{0.65}Al_{0.35}As QWs for various values of hydrostatic pressure. Theoretical results were obtained for $B = 1$ T. Solid and dashed lines correspond to the $g_{||}$ and g_{\perp} factors, respectively. Open squares, circles, and triangles correspond to the g_{\perp} factors reported in [11, 12], and [13], respectively, whereas full circles and triangles correspond to the $g_{||}$ -factor experimental measurements from [12] and [13], respectively, at low values of applied magnetic fields and zero hydrostatic pressure.

cases, and to a decrease of the g -factor anisotropy, as we have shown in figure 6 for GaAs–Ga_{0.65}Al_{0.35}As QWs. It is well known that, as the hydrostatic pressure is increased, a crossover between the Γ and X points at the Ga_{1-x}Al_xAs barriers takes place, leading to a modification of the electron-confining potential, with height behaving as a decreasing function of the applied hydrostatic pressure [20, 24, 29]. The effects of the Ga_{1-x}Al_xAs barriers become unimportant in this case and the anisotropy imposed by the confining potential falls. The same situation may be reached by increasing the QW width. When the QW width is increased, the electron wavefunction tends to localize in the GaAs region, and the influence of the barriers becomes negligible. Therefore, for large values of the hydrostatic pressure and QW width one may expect a quite small g -factor anisotropy (cf figure 6). One may note from figure 6 the fair agreement between present theoretical results for the g -factor anisotropy and the experimental data reported by Malinowski and Harley [13] and obtained for low values of the applied magnetic field and zero hydrostatic pressure.

The study of the hydrostatic-pressure effects on the conduction-electron Landé factor in semiconductor heterostructures has a valuable importance in the study of charged excitations known as charged spin-texture excitations or skyrmions [23]. Such excitations take place mainly at very small Zeeman energies. Of course, the Zeeman energy may be controlled by tuning the effective Landé factor of the system via a change of the structural parameters in the heterostructure, doping, applied external fields, or—as in [23]—by applying hydrostatic pressure. Both in the integer and fractional quantum Hall effects, it is known that, for a filling factor $\nu = n_e h / e B = 1$ (n_e is the electron density of the two-dimensional electron gas, h is the Planck constant, and e is

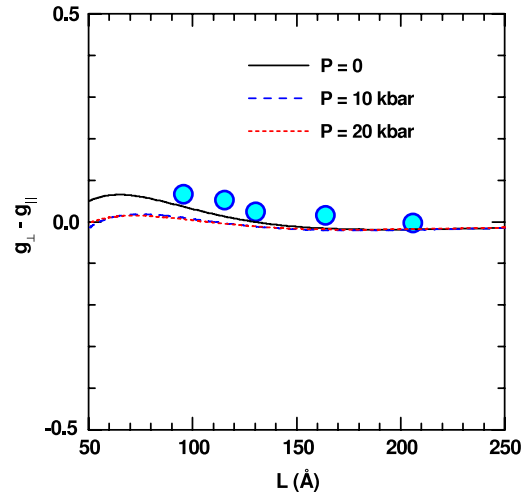


Figure 6. The anisotropy of the electron g factor, as a function of the GaAs–Ga_{0.65}Al_{0.35}As-well width, for $B = 1$ T and different values of hydrostatic pressure. Open circles correspond to $P = 0$ experimental data from Malinowski and Harley [13].

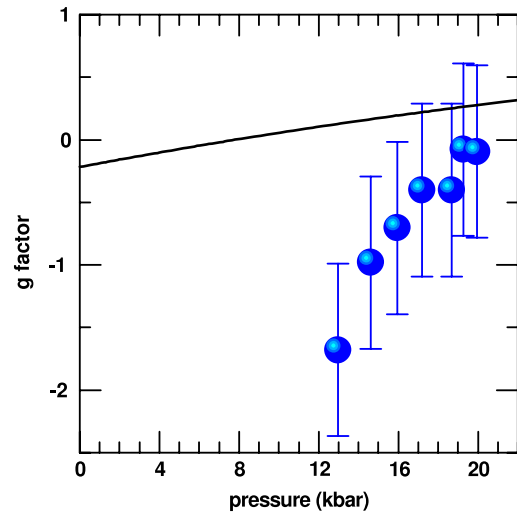


Figure 7. Hydrostatic-pressure dependence of the conduction-electron Landé factor in a 40 nm width GaAs–Ga_{0.7}Al_{0.3}As QW for a filling factor $\nu = 1$. The solid line corresponds to the present theoretical calculations whereas solid dots were obtained from the experimental measurements reported by Leadley *et al* [23].

the absolute value of the electron charge), the spin gap is given by [39]

$$\Delta = g_0 \mu_B B + E_{ex} = g^* \mu_B B, \quad (13)$$

where E_{ex} is many-body exchange energy. We have used the experimental measurements of the spin gap, reported in [23] for $\nu = 1$ in a 40 nm width GaAs–Ga_{0.7}Al_{0.3}As QW, to calculate the effective Landé factor according to expression (13). Experimental measurements of the effective Landé factor as a function of the hydrostatic pressure (solid circles) were compared with present theoretical calculations (solid line) and displayed in figure 7. Discrepancies between experimental and theoretical results may be understood in terms of the high electron density ($n_e = 0.44 \times 10^{15} \text{ m}^{-2}$)

in the experimental sample [23]. Our theoretical procedure is only valid at the limit of very low electron densities, in such a way that the exchange interaction associated with the electron gas may be ignored. However, for the electron-density value used in the experimental measurements, the effect of the exchange energy on the effective Landé factor is quite important and leads to an enhancement of the effective Landé factor. Although the agreement between experimental and theoretical results is poor, we have chosen to present these results in the hope of motivating the scientific community to perform new measurements devoted to the study of the hydrostatic-pressure dependence of the effective Landé factor in semiconductor heterostructures.

4. Conclusions

Summing up, we have studied the effects of applied hydrostatic pressure on the electron Landé g_{\parallel} factor and g -factor anisotropy in semiconductor GaAs–Ga_{1-x}Al_xAs QWs, under in-plane and growth-direction applied magnetic fields, by taking into account the non-parabolicity and anisotropy of the conduction band. Results show that the applied hydrostatic pressure increases significantly the value of both the electron g_{\parallel} and g_{\perp} factors in GaAs–Ga_{1-x}Al_xAs QWs. Finally, good agreement between the present numerical calculations and experimental measurements for the effective g factor and g -factor anisotropy was obtained in the absence of hydrostatic pressure and for low values of the magnetic field. Present theoretical results indicate that the application of hydrostatic pressure may be an invaluable tool in opening up new ways for manipulating the electron g factor in semiconductor heterostructures, a possibility of great importance in the development of spintronic devices.

Acknowledgments

We are grateful to F Culchac and A Latgé for their valuable comments and suggestions. The authors would like to thank the Brazilian Agencies CNPq, FAPESP, FAPERJ, MCT-Millennium Institute for Quantum Information, and MCT-Millennium Institute for Nanotechnology, and Colombian Agencies CODI-Universidad de Antioquia and the Excellence Center for Novel Materials and COLCIENCIAS under contract No 043-2005, for partial financial support. NPM, CAD, and ERG wish to thank the Instituto de Física, UNICAMP, Brazil, where part of this work was performed, for warm hospitality.

References

- [1] Das Sarma S 2001 *Am. Sci.* **89** 516
- [2] Žutić I, Fabian J and Das Sarma S 2001 *Appl. Phys. Lett.* **79** 1558
- [3] Žutić I, Fabian J and Das Sarma S 2004 *Rev. Mod. Phys.* **76** 323
- [4] Fabian J, Žutić I and Das Sarma S 2004 *Appl. Phys. Lett.* **84** 85
- [5] Fabian J, Matos-Abiague A, Ertler C, Peter S and Žutić I 2007 *Acta Phys. Slovaca* **57** 565
- [6] Žutić I and Fabian J 2007 *Nature* **447** 269
- [7] Weisbuch C and Hermann C 1977 *Phys. Rev. B* **15** 816
- [8] Hermann C and Weisbuch C 1977 *Phys. Rev. B* **15** 823
- [9] Oestreich M and Rühle W W 1995 *Phys. Rev. Lett.* **74** 2315
- [10] Oestreich M, Hallstein S, Heberle A P, Eberl K, Bauser E and Rühle W W 1996 *Phys. Rev. B* **53** 7911
- [11] Hannak R M, Oestreich M, Heberle A P, Rühle W W and Kohler K 1995 *Solid State Commun.* **93** 319
- [12] Le Jeune P, Robart D, Marie X, Amand T, Brosseau M, Barrau J, Kalevcih V and Rodichev D 1997 *Semicond. Sci. Technol.* **12** 380
- [13] Malinowski A and Harley R T 2000 *Phys. Rev. B* **62** 2051
- [14] Heberle A P, Rühle W W and Ploog K 1994 *Phys. Rev. Lett.* **72** 3887
- [15] Yugova I A, Greilich A, Yakovlev D R, Kiselev A A, Bayer M, Petrov V V, Dolhikh Yu K, Reuter D and Weick A D 2007 *Phys. Rev. B* **75** 245302
- [16] Pfeffer P and Zawadzki W 2006 *Phys. Rev. B* **74** 115309
- [17] Pfeffer P and Zawadzki W 2006 *Phys. Rev. B* **74** 233303
- [18] Venkateswaran U, Chandrasekhar M, Chandrasekhar H R, Vojak B A, Chambers F A and Meese J M 1986 *Phys. Rev. B* **33** 8416
- [19] Satpathy S, Chandrasekhar M, Chandrasekhar H R and Venkateswaran U 1991 *Phys. Rev. B* **44** 11339
- [20] Burnett J H, Cheong H M, Paul W, Koteles E S and Elman B 1993 *Phys. Rev. B* **47** 1991
- [21] Ogg N R 1966 *Proc. Phys. Soc.* **89** 431
- [22] McCombe B O 1969 *Phys. Rev.* **181** 1206
- [23] Leadley D R, Nicholas R J, Maude D K, Utjuzh A N, Portal J C, Harris J J and Foxon C T 1998 *Semicond. Sci. Technol.* **13** 671
- [24] Reyes-Gómez E, Raigoza N and Oliveira L E 2008 *Phys. Rev. B* **77** 115308
- [25] Golubev V G, Ivanov-Omskii V I, Minervin I G, Osutin A V and Polyakov D G 1985 *Sov. Phys.—JETP* **61** 1214
- [26] Dresselhaus G 1955 *Phys. Rev.* **100** 580
- [27] Reyes-Gómez E, Porras-Montenegro N, Perdomo-Leiva C A, Brandi H S and Oliveira L E 2008 *J. Appl. Phys.* **104** 023704
- [28] de Dios-Leyva M, Lopez-Gondar J and del Valle J S 1988 *Phys. Status Solidi b* **148** K113
- [29] del Valle J S, Lopez-Gondar J and de Dios-Leyva M 1989 *Phys. Status Solidi b* **151** 127
- [30] Elabsy A M 1994 *J. Phys.: Condens. Matter* **6** 10025
- [31] Cheong H M, Burnett J H, Paul W, Hopkins D F, Campman K and Gossard A C 1996 *Phys. Rev. B* **53** 10916
- [32] Goñi A R, Syassen K, Strössner K and Cardona M 1989 *Semicond. Sci. Technol.* **4** 246
- [33] Wolford D J, Keuch T F, Bradley J A, Gell M A, Ninno D and Jaros M 1986 *J. Vac. Sci. Technol. B* **4** 1043
- [34] Gell M A, Ninno D, Jaros M, Wolford D J, Keuch T F and Bradley J A 1987 *Phys. Rev. B* **35** 1196
- [35] de Dios-Leyva M, Reyes-Gómez E, Perdomo-Leiva C A and Oliveira L E 2006 *Phys. Rev. B* **73** 085316
- [36] Reyes-Gómez E, Perdomo-Leiva C A, de Dios-Leyva M and Oliveira L E 2006 *Phys. Rev. B* **74** 033314
- [37] López F E, Rodríguez B A, Reyes-Gómez E and Oliveira L E 2008 *J. Phys.: Condens. Matter* **20** 175204
- [38] de Dios-Leyva M, Porras-Montenegro N, Brandi H S and Oliveira L E 2006 *J. Appl. Phys.* **99** 104303
- [39] Dobers M, Klitzing K v and Weimann G 1988 *Phys. Rev. B* **38** 5453
- [40] Liang C-T, Cheng Y-M, Huang T Y, Huang C F, Simmons M Y, Ritchie D A, Kim G-H, Leem J Y, Chang Y H and Chen Y F 2001 *J. Phys. Chem. Solids* **62** 1789